Hysteresis of gating underlines sensitization of TRPV3 channels

Beiying Liu,[1] Jing Yao,[1] Michael X. Zhu,[2] and Feng Qin[1]

[1]Department of Physiology and Biophysical Sciences, State University of New York at Buffalo, Buffalo, NY 14214
[2]Department of Integrative Biology and Pharmacology, The University of Texas Health Science Center at Houston, Houston, TX 77030

Vanilloid receptors of the transient receptor potential family have functions in thermal sensation and nociception. Among them, transient receptor potential vanilloid (TRPV)3 displays a unique property by which the repeated stimulation causes successive increases in its activity. The property has been known as sensitization and is observed in both native cells and cells heterologously expressing TRPV3. Transient increases in intracellular calcium levels have been implicated to play a key role in this process by mediating interaction of calmodulin with the channel. In support of the mechanism, BAPTA, a fast calcium chelator, accelerates the sensitization, whereas the slow chelator EGTA is ineffectual. Here, we show that the sensitization of TRPV3 also occurred independently of Ca^{2+}. It was observed in both inside-out and outside-out membrane patches. BAPTA, but not EGTA, has a direct potentiation effect on channel activation. Analogues of BAPTA lacking Ca^{2+}-buffering capability were similarly effective. The stimulation-induced sensitization and the potentiation by BAPTA are distinguishable in reversibility. We conclude that the sensitization of TRPV3 is intrinsic to the channel itself and occurs as a result of hysteresis of channel gating. BAPTA accelerates the sensitization process by potentiating the gating of the channel.

INTRODUCTION

Transient receptor potential vanilloid (TRPV)1–4 are commonly activated by temperature with activation thresholds coinciding with the physiological thermal thresholds of peripheral sensory nerve fibers. Among them, TRPV1 and TRPV2 have been suggested to mediate nociception above 40 and 50°C, respectively (Caterina et al., 1997, 1999), whereas TRPV3 and TRPV4 are responsible for warm sensation (27–42°C) (Peier et al., 2002; Smith et al., 2002; Xu et al., 2002). The vanilloid receptors constitute a subgroup in the large transient receptor potential superfamily. They have a membrane topology similar to voltage-gated K^+ channels, with six transmembrane segments (S1–S6) and a reentrant pore loop between S5 and S6, but contain additional structure motifs in the two relatively large intracellular termini, notably the ankyrin repeats on the N terminus. Animals lacking TRPV1 and TRPV3 are deficient in thermal sensation and heat-induced hyperalgesia, supporting their roles in thermal sensation and nociception (Caterina et al., 2000; Davis et al., 2000; Moqrich et al., 2005).

Besides thermal stress, the TRPVs respond to stimuli of other modalities, in particular, the chemical cues that are correlated to thermal perception. For example, capsaicin, the pungent ingredient of chili peppers, activates TRPV1 to give rise to a hot or burning sensation. Oregano, savory, and thyme have actions on TRPV3 to evoke a sense of warmth (Xu et al., 2006). The expression of TRPV3 is found in skin keratinocytes and tongue and nose epithelium cells. Thus, its chemosensitivity has also been linked to flavor sensations of plant derivatives as well as skin sensitization.

Despite a sequence homology to other vanilloid receptors, TRPV3 exhibits a unique, somewhat unusual property known as sensitization, by which the repeated application of a stimulus leads to progressive increases in its response (Peier et al., 2002; Xu et al., 2002; Chung et al., 2004). Before sensitization, the channel generally shows only a small activity. This sensitization behavior appears to occur regardless of the modality of the stimulus and is observed in both native and heterologously expressing cells. One mechanism that has been put forward involves Ca^{2+}-mediated interactions between calmodulin (CaM) and the channel (Xiao et al., 2008; Phelps et al., 2010). Ca^{2+} binding to CaM causes inhibition of the channel. Agonists such as 2-APB can induce intracellular Ca^{2+} rises via cell surface and internal TRPV3 channels. It also has nonspecific actions on other channels; for example, it antagonizes IP3 receptors (Maruyama et al., 1997), blocks gap-junctional channels (Harks et al., 2003) and affects Orai channels

B. Liu and J. Yao contributed equally to this paper.
Correspondence to Feng Qin: qin@buffalo.edu
J. Yao's present address is Key Laboratory of Molecular Biophysics of the Ministry of Education, Huazhong University of Science and Technology, Wuhan, Hubei, China.

Abbreviations used in this paper: CaM, calmodulin; TRPV, transient receptor potential vanilloid.

The Rockefeller University Press $30.00
J. Gen. Physiol. Vol. 138 No. 5 509–520
www.jgp.org/cgi/doi/10.1085/jgp.201110689

(Lis et al., 2007). One key piece of evidence for the mechanism is that the Ca^{2+} chelators with different buffering kinetics exhibit differential effects on sensitization. The fast chelator BAPTA results in a more rapid development of sensitization, whereas the slow chelator EGTA has no effect. This functional difference is correlated with the kinetic difference of Ca^{2+} chelation because BAPTA but not EGTA may rapidly buffer Ca^{2+} releases, thereby blocking the inhibition of the channel by CaM.

Here, we show that the sensitization of TRPV3 observed in intact cells is reproducible in excised membrane patches. We found that the gating of the channel itself exhibits strong hysteresis causing the apparent sensitization. BAPTA exerts a direct effect on the channel by potentiating channel activation. The sensitization induced by repeated stimulation and the potentiation by BAPTA are distinguishable in that the sensitization is irreversible while the potentiation effect is readily washable. In further support of Ca^{2+} independence, we found that synthetic dipeptides that are structurally similar to BAPTA but incapable of Ca^{2+} binding can also both potentiate channel gating and accelerate sensitization. Our results reveal that the gating of transient receptor potential channels can be plastic undergoing irreversible structural adaptations.

MATERIALS AND METHODS

Cell culture and expression

HEK 293 cells were grown in Dulbecco's modified Eagle's medium containing 10% fetal bovine serum (Hyclone Laboratories, Inc.) and 1% penicillin/streptomycin and were incubated at 37°C in a humidified incubator gassed with 5% CO_2. Transfection was made at a confluence of ∼80% by calcium phosphate precipitation. Monomeric red fluorescent protein (mRFP) was cotransfected for laser beam positioning. Experiments took place usually 10–28 h after transfection. mTRPV3 was provided by A. Patapoutian (The Scripps Research Institute, San Diego, CA).

Electrophysiology

Patch-clamp recording was made in whole cell and excised patch configurations. Currents were amplified using an Axopatch 200B amplifier (Axon Instruments), low-pass filtered at 5–10 kHz through the built-in eight-pole Bessel filter, and sampled at 10–20 kHz with a multifunctional data acquisition card (National Instruments). Data acquisition was controlled by custom-made software, which was capable of synchronous I/O and simultaneous control of laser and patch-clamp amplifier. Patch pipettes were fabricated from borosilicate glass capillary (Sutter Instrument) and fire-polished to a resistance of <5 MΩ when filled with 150 mM CsCl solution. Pipette series resistance and capacitance were compensated using the built-in circuitry of the amplifier (50–70%), and the liquid junction potential between the pipette and bath solutions was zeroed before seal formation. Currents were evoked from a holding potential of ±60 mV.

Bath solutions for whole cell recording consisted of (mM): 150 NaCl, 5 EGTA, and 10 HEPES, pH 7.4 (adjusted with NaOH). Electrodes were filled with (mM): 140 CsCl, 10 HEPES, and 1 EGTA, pH 7.4 (adjusted with CsOH). For excised patches, symmetric solutions of 150 NaCl were used. When BAPTA was used, it replaced EGTA in the pipette (whole cell) or perfusion (excised patch) solutions. The pH of the HEPES-buffered solutions changed by ≤0.4 unit over 22–55°C. Chemicals including CaM inhibitors calmidazolium and W-7 were purchased from Sigma-Aldrich. Ophiobolin A was from VWR International. Synthetic peptides were from AnaSpec.

Temperature jump

Temperature jumps were produced by laser irradiation as described previously (Yao et al., 2010). In brief, a single emitter infrared laser diode was used as a heat source. Laser emission from the diode was launched into a multimode fiber with a 100-µm core diameter and 0.2 NA. The other end of the fiber was positioned close to cells as the perfusion pipette normally was. The laser diode was driven by a pulsed quasi-CW current power supply (Lumina Power). Pulsing of the controller was controlled from computer through the data acquisition card using a custom program. A green laser line (532 nm) was coupled to the fiber to aid alignment. The beam spot on the coverslip was identified by illumination of mRFP-expressing cells.

Constant temperature steps were generated by irradiating the tip of an open pipette and using the current of the electrode as the readout for feedback control. The laser was first powered on for a brief duration to reach the target temperature and was then modulated to maintain a constant pipette current. The sequence of the modulation pulses was stored and subsequently played back to apply temperature jumps to whole cells or membrane patches. Temperature was calibrated offline from the pipette current using the temperature dependence of electrolyte conductivity.

Online supplemental material

Fig. S1 shows the sensitization of TRPV3 resulting from sustained stimulation and compares it with the sensitization induced by repetitive stimulation. It is available at http://www.jgp.org/cgi/content/full/jgp.201110689/DC1.

RESULTS

Sensitization of TRPV3 and its dependence on Ca^{2+} chelators

We first examined the sensitization of TRPV3 and the effects of Ca^{2+} chelators using a stimulation protocol as reported previously (Xiao et al., 2008). Fig. 1 A illustrates whole cell currents recorded from transiently transfected HEK 293 cells (V_h = −60 mV). The agonist (30 µM 2-APB) was applied repeatedly, with each exposure lasting for ∼15 s followed by a complete washout (with the bath solution). The response generally did not reach a steady state within each stimulation, so we compared the peak response at the end of each exposure. The channel activity was initially small (∼9 pA/pF) but grew steadily in subsequent stimulations. In general, this increase of response developed over a period of many minutes (∼10 min) before saturating. The time course tended to be sigmoidal or sublinear. The extent of the change was quite dramatic (∼94-fold).

The sensitization of the channel was also observed with heat activation. Fig. 1 B shows the temperature response of TRPV3 after repeated stimulation by a same-temperature jump from room temperature to ∼53°C. Each temperature jump had a rise time of 0.75 ms and

lasted for 100 ms. The repetition resulted in a progressive increase in the heat response (approximately fourfold). Fig. 1 C compares the activation time course over successive jumps. The current rose approximately linearly with time upon initial stimulation. After sensitization, the activation became exponential. The half-time ($t_{1/2}$) of activation decreased from ~29 to 8 ms ($n = 10$). The sensitization was thus accompanied with marked changes in activation kinetics in addition to peak responses. It occurs regardless of the modality of the stimulus.

Our above experiments were conducted with 5 mM EGTA in the pipette solution (no Ca^{2+} in bath, pipette, and perfusion solutions). We further examined the sensitization using another Ca^{2+} chelator, BAPTA. Fig. 1 D shows the resulting 2-APB responses, which also increased progressively over repeated stimulations (30 μM, same as in Fig. 1 A). Notably, the sensitization became more rapid. The peak current increased superlinearly with time (Fig. 1 G) and reached saturation approximately twice as fast as with EGTA. In addition, the initial 2-APB activity appear to be much larger (EGTA: 9 ± 3 pA/pF, $n = 10$; BAPTA: 248 ± 144 pA/pF, $n = 16$), so that the actual increase of the current before and after sensitization is considerably less than with EGTA (Fig. 1 H). Similar changes were observed with heat responses (Fig. 1, E, F, I, and J). The initial response, relative to the final sensitized response, was ~72% as compared with ~27% when EGTA was used.

Sensitization is membrane delimited

To discern whether the sensitization is dependent on intracellular signaling, we repeated the experiments in excised membrane patches. Fig. 2 A shows the response of the channel to 30 μM 2-APB recorded from an outside-out patch at −60 mV. The pipette solution contained 5 mM EGTA. The current was initially small (~126 pA) but increased with repeated stimulation. The final response reached ~2 nA, giving an ~20-fold

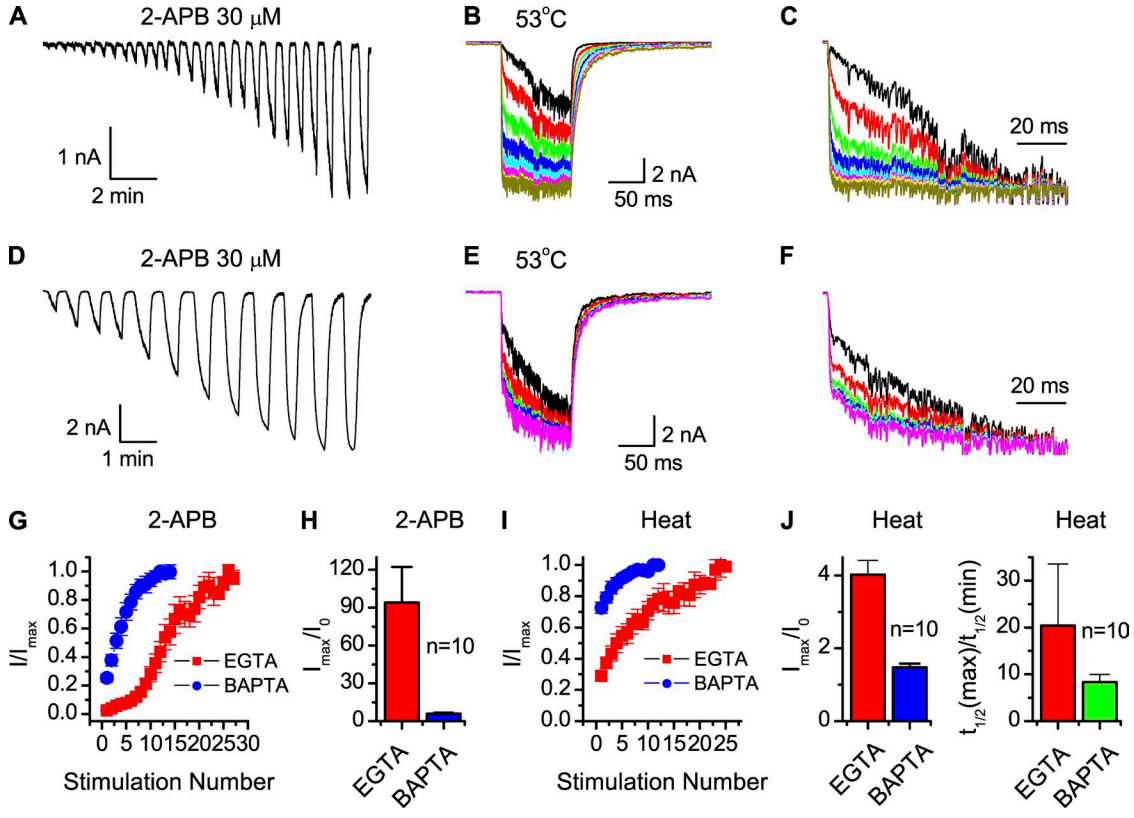

Figure 1. Sensitization of TRPV3 in intact cells. (A) Exemplar trace of channel activity evoked by repeated application of 30 μM 2-APB. (B) Heat-evoked currents in response to repeated temperature jumps (temperature was stepped from room temperature to 53°C in 0.75 ms and then clamped for 100 ms). (C) Normalized heat response showing the change of the activation time course in successive stimulations (each trace was normalized by its own maximum response). (D–F) Parallel recordings of 2-APB (D) and heat (E and F) responses using 5 mM BAPTA instead of EGTA for intracellular Ca^{2+} buffering. (G–J) Time course and extent of sensitization using different Ca^{2+} chelators: (G and H) 2-APB; (I and J) heat. For the time course, currents were normalized by the maximum values after sensitization. For the extent of sensitization, the relative increase of currents obtained during the first and the last stimulation was plotted. For the half-time ($t_{1/2}$) plot, the ratio for the half-activation time of the last stimulation to the first one was shown. Recordings were from transiently transfected HEK 293 cells held at −60 mV. The pipette solution contained 5 mM EGTA (A and B) or 5 mM BAPTA (D and E). The extracellular solution is Ca^{2+} free (buffered with 5 mM EGTA).

increase before and after sensitization (Fig. 2 J). The heat activation (53°C) was similarly sensitized. The first temperature jump produced a small and slowly developed current ($t_{1/2}$ of ~33 ms, I_{max} of ~820 pA). After sensitization, the activation was accelerated to $t_{1/2}$ = 5 ms, and the peak response was increased to ~5 nA. These changes were reminiscent of those in whole cell experiments. In the outside-out configuration, the sensitization of the 2-APB response took ~17 repetitions (each ~15 s) (Fig. 2 I) and the heat response took ~20 exposures (each 100 ms) (Fig. 2 K), comparable to those in the whole cell condition.

The differential effects of BAPTA and EGTA were also observed in isolated patches. Fig. 2 (C and D) shows 2-APB and heat responses from outside-out patches with 5 mM BAPTA in the pipette solution. The sensitization of the 2-APB response took three to four stimulations to reach a half-maximum value (Fig. 2 I), whereas the heat response (53°C) needed two to three repetitions (Fig. 2 K). Both responses were sensitized more rapidly than when EGTA was used. After sensitization, the peak current of the channel was increased, respectively, by approximately fivefold for 2-APB and ~1.5-fold for heat (Fig. 2, J and L). These changes were also consistent with the respective whole cell measurements.

To further ensure that the excised membrane patches are free of intracellular Ca^{2+} stores, we repeated the experiments in the inside-out configuration so that the cytosolic face of the membrane is accessible to direct washout. As illustrated in Fig. 2 (E–H), these experiments resulted in similar observations to those in outside-out recordings. Both 2-APB and heat responses remained sensitized regardless of Ca^{2+} chelators (EGTA: 48 ± 13–fold for 2-APB, n = 15, and 7 ± 1–fold for heat, n = 4; BAPTA: 11 ± 4–fold for 2-APB, n = 11, and ~1.5-fold for heat, n = 6). BAPTA caused more rapid sensitization and a larger initial response (Fig. 2, I–L).

Sensitization involves hysteresis of gating

The above experiments suggest that the sensitization of TRPV3 does not require the whole cell environment. Instead, it appears to be intrinsic to the channel itself. To distinguish whether the sensitization results from changes in gating or conductance, we measured single-channel activity. Fig. 3 A shows unitary currents in response to 2-APB in an outside-out patch before and after sensitization (induced by repeated applications of 300 µM 2-APB, which sensitized the channel more rapidly than 30 µM 2-APB, as illustrated in Fig. 3 J). The i-V curves virtually overlap (Fig. 3 B), indicating

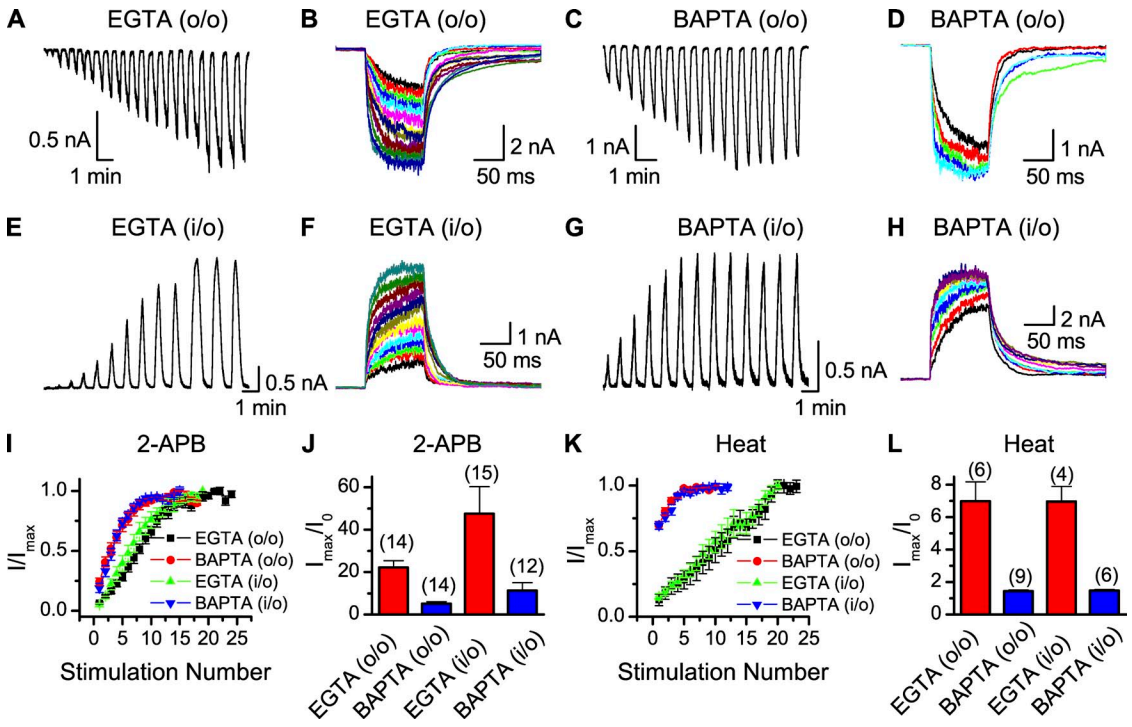

Figure 2. Sensitization of TRPV3 in membrane patches. (A and B) Current traces recorded in outside-out configuration, evoked by repeated applications of 30 µM 2-APB (A) or fast temperature jumps (53°C; B). The pipette solution contained 5 mM EGTA. (C and D) Similar recordings but with 5 mM BAPTA instead of EGTA. (E–H) Recordings of sensitization in inside-out patches. (E and F) 5 mM EGTA. (G and H) 5 mM BAPTA. The chelators were included in the perfusion solution. (I–L) Summary plots of time course and extent of sensitization: (I and J) 2-APB response; (K and L) heat response. Membrane patches were excised from TRPV3-expressing HEK 293 cells. Hold potential was −60 mV (outside-out) and +60 mV (inside-out).

that the sensitization results from changes in gating, not conductance.

To quantify the gating change, we measured the temperature response curve of TRPV3. Fig. 3 (C–E) illustrates temperature responses in an inside-out membrane patch evoked by a family of temperature jumps ranging from 30 to 54°C. Before sensitization, the activation was slow and had a relatively high threshold (>40°C). After sensitization (induced by repeated jumps to 53°C), significant activity started at ~30°C. The threshold of activation was considerably reduced. Fig. 3 F plots the temperature dependence of the current. Before sensitization, the curve follows two linear fits where the fit in the high temperature range was strongly temperature dependent, reflecting the gating of the channel, whereas the fit in the low temperature range corresponds to the leakage current. From the slope of the fit we estimated a temperature coefficient of the channel at about Q_{10} of ~39. After sensitization, the temperature coefficient was reduced to Q_{10} of ~4. The sensitization of the channel thus involves a profound reduction in the temperature dependence in addition to the threshold of activation, suggesting that its occurrence was accompanied with substantial structural changes.

The sensitization, albeit influenced by BAPTA, occurred regardless of whether Ca^{2+} chelators were used. Fig. 3 (G–I) shows the 2-APB response from an inside-out patch recorded without the addition of either EGTA or BAPTA in the pipette solution. By repeated applications of 30 μM 2-APB, the channel remained sensitized progressively as occurred in the presence of Ca^{2+} chelators. The time course of the sensitization tended to be

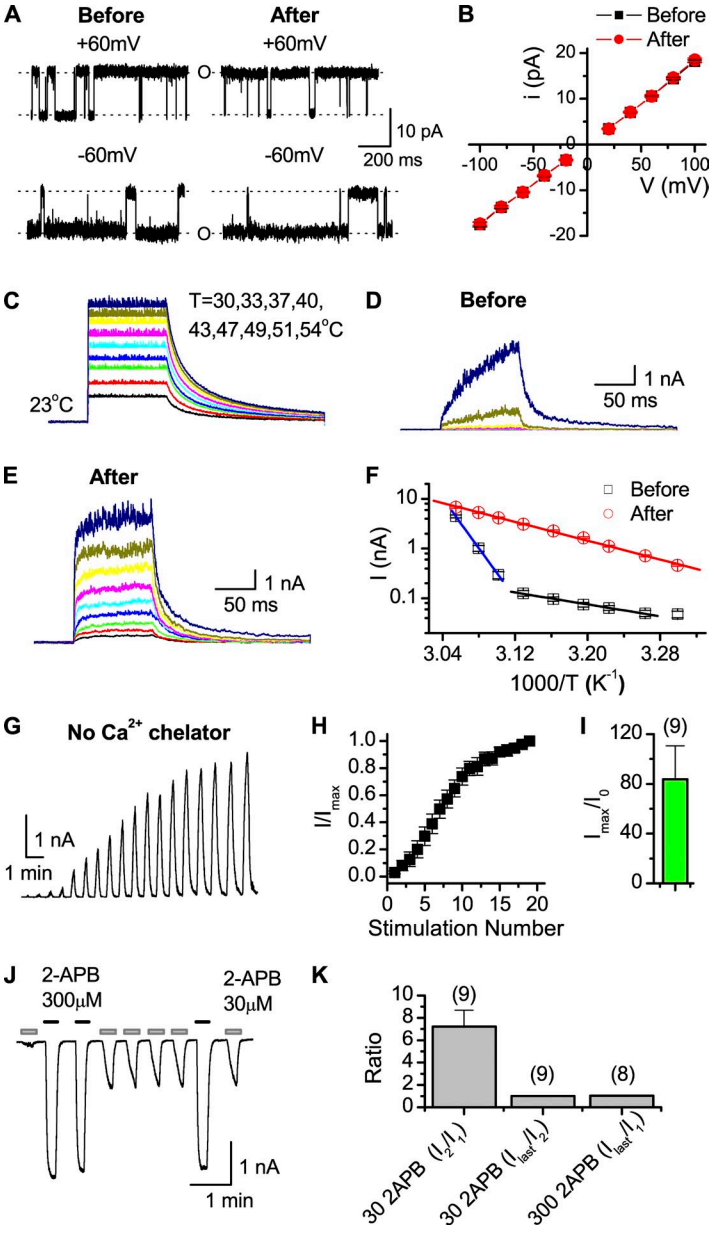

Figure 3. Sensitization is gating dependent. (A and B) Single-channel currents of TRPV3, showing no significant change in the unitary conductance of the channel before and after sensitization. Currents were evoked by 10 and 3 μM 2-APB, respectively, before and after sensitization and were from inside-out membrane patches of HEK 293 cells at the indicated potentials. Sensitization was induced with 300 μM 2-APB. (C–F) Heat-evoked currents and their temperature dependence before and after sensitization: (C) temperature jumps (30–54°C); (D) responses at control (before sensitization); (E) responses to same temperature jumps after sensitization (induced by repeated temperature stimulation at 53°C); and (F) temperature dependence before and after sensitization. Linear fits: Q_{10} of ~65 (before) and ~4 (after). The fit for the leakage at control in the low temperature region had Q_{10} of ~2. Data were recorded from inside-out patches at +60 mV. (G–I) Sensitization in the absence of Ca^{2+} chelators. Currents were in response to 30 μM 2-APB recorded from an inside-out patch at +60 mV. The perfusate was free of EGTA and BAPTA. (J and K) Sensitization induced by a single application of 2-APB at a supramaximal concentration (300 μM). A subsequent application of 300 μM 2-ABP ensured that the channel was fully sensitized. After sensitization, the channel exhibited stable responses to repeated applications of 2-APB at a submaximal concentration (30 μM). Recordings were made in outside-out patches at −60 mV.

sigmoidal, resembling that with EGTA (Fig. 3 H), although the extent appeared larger (Fig. 3 I). The heat response was similarly sensitized (not depicted). These data indicate that Ca^{2+} chelators are not necessary for the occurrence of sensitization.

The sensitization appears to be activity dependent and independent of stimulation protocol. Instead of repeated brief stimulation, we tested the sensitization with a single prolonged application of 2-APB at a supermaximal concentration. Fig. 3 J illustrates such a continuous treatment with 300 µM 2-APB in an outside-out patch. At this relatively high concentration, the response of the channel increased steadily until saturation. After the treatment, the channel became significantly more responsive to 2-APB at lower concentrations (e.g., 30 µM), confirming that it was indeed sensitized. Furthermore, the repeated application of 2-APB at either high or low concentrations did not incur further increases in responses (Fig. 3, J and K), indicating that the gating did not undergo further hysteresis. Prolonged stimulation at low concentrations was also able to sensitize the channel (Fig. S1), although it took a much longer duration, on the order of several minutes. This time course was similar to that when the same concentration of agonist was applied repetitively, suggesting that the sensitization involves slow activation of the channel. The extent of the sensitization, estimated as the increase of the current relative to the initial response, was also comparable. Thus, the prolonged stimulation was equally effective as the repeated brief stimulation in sensitizing the channel. That the sensitization does not require Ca^{2+}-buffering reagents and is independent of the stimulation protocol indicates that the sensitization is intrinsic to the gating of the channel itself.

BAPTA potentiates channel activation

To understand how BAPTA contributes to sensitization, we examined whether it has a direct effect on channel gating. Fig. 4 A shows its effects on the 2-APB response in an inside-out patch. Here, we first sensitized the channel by repeated stimulation with 100 µM 2-APB. After sensitization, we tested the response to 30 µM 2-APB with and without the addition of 10 mM BAPTA. The presence of BAPTA considerably increased the 2-APB response. Furthermore, after washing off BAPTA, 2-APB (BAPTA-free) invoked a similar response to that before BAPTA treatment (Fig. 4 B), suggesting that the potentiation effect of BAPTA is reversible. This is contrary to the sensitization, which appeared irreversible and lasted for the whole experimental time (>10 min). BAPTA (up to 30 mM) alone did not activate the channel.

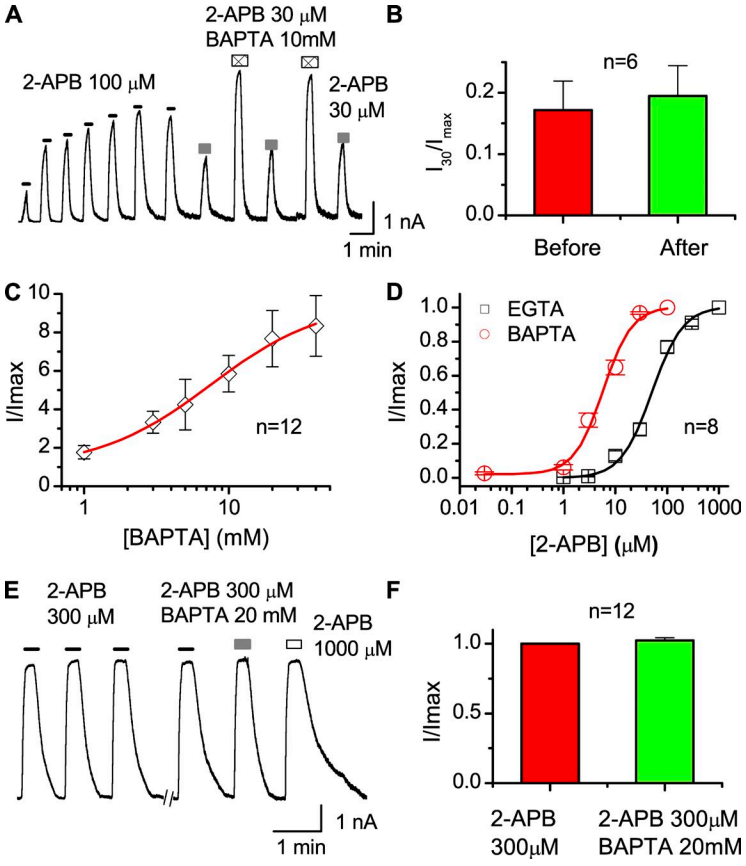

Figure 4. Direct effects of BAPTA on gating. (A and B) BAPTA potentiates 2-APB response in a reversible manner. After sensitization by repeated application of 100 µM 2-APB, the channel was exposed to 30 µM 2-APB with or without 10 mM BAPTA. The average plot compares the 2-APB response (30 µM) before and after BAPTA treatment. (C) Dose dependence of BAPTA effects on 2-APB response (30 µM). The solid line corresponds to a partial fit by Hill's equation with EC_{50} = 7.5 ± 1.3 mM and n_H = 1.1 ± 0.3 (n = 12). The BAPTA effects were measured after full sensitization of the channel by repeated stimulation with 2-APB as shown in A. (D) Dose–response curves of 2-APB (black, EGTA; red, BAPTA). The solid lines are fits to Hill's equations with EC_{50} = 51 ± 11 µM and n_H = 1.5 ± 0.3 for EGTA and EC_{50} = 6 ± 2 µM and n_H = 1.6 ± 0.3 for 10 mM BAPTA. (E and F) Representative current trace showing that BAPTA does not alter the maximum attainable response of 2-APB. 300 µM 2-APB was first applied to sensitize the channel and subsequently combined with 20 mM BAPTA for the potentiated response. At the end, 1 mM 2-APB was applied to ensure the attainment of a maximum response. All recordings were from inside-out membrane patches of HEK 293 cells held at +60 mV.

Because the potentiation effect of BAPTA was reversible, we examined it in more mechanistic detail. Fig. 4 C shows its concentration dependence (measured after the channel was sensitized). The potentiation of the 2-APB response (30 μM) was increased in a concentration-dependent manner. BAPTA was effective above 1 mM and remained effective up to 40 mM with a half-maximal concentration of ∼8 mM. Fig. 4 D shows the change of the dose–response curve of 2-APB. The application of 10 mM BAPTA left-shifted the 2-APB response curve with EC_{50} reduced by approximately ninefold (control/EGTA: ∼51 μM; BAPTA: ∼6 μM). The steepness of the curve remains largely unchanged (control: n_H of ∼1.5; BAPTA: ∼1.6).

To determine whether BAPTA affects gating efficacy, we measured the maximum response of 2-APB (Fig. 4, E and F). After sensitization, 300 μM 2-APB produced a maximum response (similar to that of 1,000 μM 2-APB). The addition of BAPTA did not further increase the response. This is observed for a range of BAPTA concentrations (5–20 mM). Thus, BAPTA mainly exerts an effect on the sensitivity of the channel and does not impact the efficacy of gating.

The heat response of the channel was also strongly affected by BAPTA. Fig. 5 A shows the heat-evoked current (51 and 54°C) from channels that have been pre-sensitized. The addition of BAPTA considerably increased the response, whereas the subsequent washout of BAPTA restored the response before BAPTA treatment. Thus, the potentiation effects of BAPTA on the heat activation were also reversible.

We quantified the effects of BAPTA on the temperature dependence of the channel (Fig. 5, B and C). In these experiments, the channel was first sensitized by repeated exposures to 100-ms-long temperature jumps (50°C). After sensitization, we measured the heat-evoked currents in response to a family of temperature jumps ranging from 34 to 51°C. The resulting temperature response curves showed similar slope sensitivity with or without the addition of BAPTA (Fig. 5 C). At control, a linear fit of the curve resulted in ΔH of ∼23 kcal/mol, whereas in the presence of BAPTA, the fit gave rise to ΔH of ∼27 kcal/mol. Hence, BAPTA did not perturb the intrinsic temperature dependence of the channel, which is contrary to the sensitization effect on the channel. The effects of BAPTA on both 2-APB and heat responses can be explained by a shift of the midpoint of the activation curve.

Pharmacophore of BAPTA

BAPTA differs from EGTA in that it contains two benzene rings, whereas EGTA has a linear structure (Fig. 6 A). 2-APB also carries two adjacent benzene rings (Fig. 6 A). We hypothesize that the benzene rings may be responsible for the potentiation effects of BAPTA. To test the hypothesis, we designed two synthetic peptides containing ring structures; one is a diphenylalanine, and the other is benzoyl-L-phenylalanine (Fig. 6 A). Fig. 6 (B–D) shows that both compounds were indeed able to potentiate the channel. 3 mM diphenylalanine increased the 2-APB response (30 μM) by approximately ninefold, whereas 100 μM benzoylphenylalanine led to an approximately fivefold potentiation. By themselves, the compounds did not evoke a significant activity. Fig. 6 (E–G) illustrates the effects of the peptides on the sensitization induced by repeated applications of 30 μM 2-APB. The sensitization also became more rapid than control where EGTA was used (Fig. 6 G). The effects of these compounds

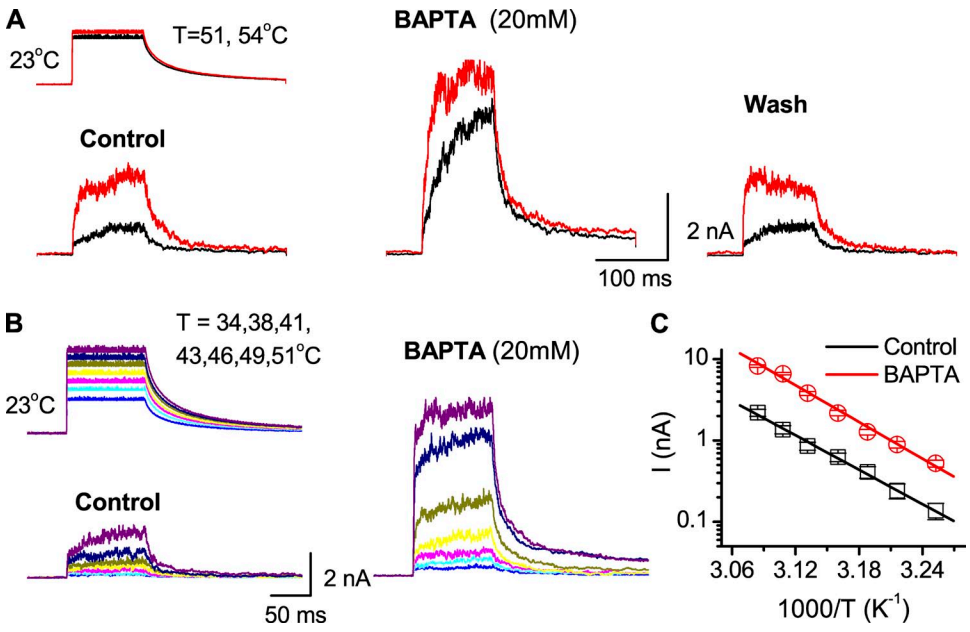

Figure 5. Effects of BAPTA on temperature gating. (A) Reversible potentiation of heat activation by BAPTA. 20 mM BAPTA was applied by brief perfusion to the patch before temperature jumps. (B and C) Effects of BAPTA on temperature dependence. Temperature jumps are shown on the top left. Linear fitting of the temperature response curves gave Q_{10} of ∼3.5 at control and ∼4.4 after the addition of 20 mM BAPTA. Recordings were from inside-out membrane patches of HEK 293 cells at +60 mV.

were thus similar to those of BAPTA, indicating that the aromatic rings of BAPTA are essential to its functions, whereas the Ca^{2+}-binding moiety is not.

DISCUSSION

The sensitization resulting from repeated stimulation is a characteristic feature of TRPV3 (Chung et al., 2004). Its differential dependence on different intracellular Ca^{2+} chelators has led to the proposition of a mechanism involving Ca^{2+}-dependent intracellular regulation of the channel (Xiao et al., 2008). In this mechanism, the elevation of intracellular Ca^{2+} after activation of TRPV3 causes activation of CaM, and the binding of CaM to the channel leads to inhibition of the channel. Such a signaling cascade can be preferentially blocked by the fast chelator BAPTA but not by the slow EGTA. Here, we have proposed an alternative mechanism independent of intracellular signaling. We suggest that the sensitization is intrinsic to the gating of the channel itself.

We have provided several lines of evidence that the sensitization of TRPV3 does not require intracellular signaling. First, it can be replicated in membrane patches at both inside-out and outside-out configurations. Such patches are presumably free of internal Ca^{2+} stores, especially for inside-out patches, which are under continuous perfusion of solutions. Second, BAPTA remained effective on accelerating sensitization in membrane patches.

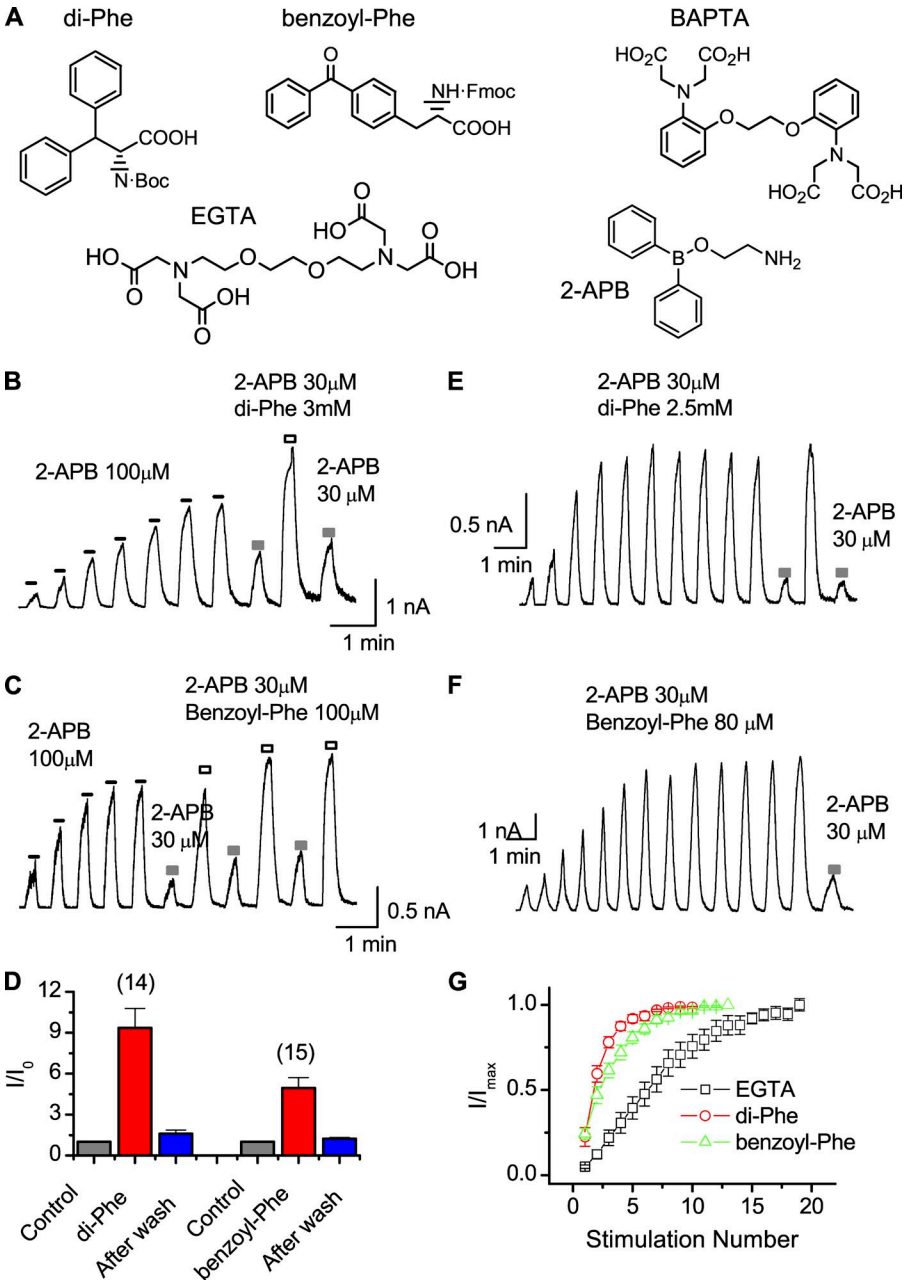

Figure 6. Pharmacophore of BAPTA. (A) Structures of the synthetic peptides Boc-D-3,3-diphenylalanine (di-PHE) and Fmoc-4-benzoyl-L-phenylalanine (benzoyl-PHE) compared with those of BAPTA, EGTA, and 2-APB. (B) Potentiation by di-PHE. The channel was first sensitized by treatments with 100 μM 2-APB, followed by the application of 30 μM 2-APB to assess the potentiation effect of the peptide and its reversibility. (C) Similar effects of benzoyl-PHE. (D) Relative changes of the 2-APB response after the addition and wash-off of the compounds. (E–G) Acceleration of sensitization by di-PHE and benzoyl-PHE. Recordings were made in the inside-out configuration from membrane patches of HEK 293 cells and were held at +60 mV.

Such effects would be difficult to explain by a Ca^{2+}-buffering mechanism because, even if intracellular Ca^{2+} stores were not completely washed off, Ca^{2+} released from these stores would be difficult to diffuse to the plasma membrane domains at a high concentration. Third, the effects of BAPTA are reversible and can be mimicked by analogues that do not have the Ca^{2+}-buffering capability, indicating that BAPTA has a direct effect on channel gating.

Our data show that the gating of TRPV3 undergoes strong hysteresis (irreversible changes). Although we do not know the exact time scale of the hysteresis, it appeared to last at least for the whole experimental time (>10 min). The functional consequences of the hysteresis involve increases in both open probability and rate of activation. These changes are parallel to the sensitization effects in intact cells. Because the hysteresis is gating or activity dependent, any modulator of the channel could potentially alter its extent or kinetics. Thus, the seeming dependence of the sensitization on different Ca^{2+} chelators can be accounted for by a direct effect of BAPTA on channel gating itself rather than buffering of intracellular Ca^{2+}.

It is of note that although our results support a membrane-delimited mechanism for the sensitization, they do not necessarily refute the regulation of the channel by intracellular signaling pathways. For example, the evidence for the modulation of the channel by CaM is compelling (Xiao et al., 2008). In vitro binding assays support a direct interaction between them. Pharmacology experiments also show that inhibiting CaM affected the channel activity. Mutagenesis data further locate the binding of CaM on the N terminus of the channel. To test whether the sensitization occurring in excised patches was a result of Ca^{2+}–CaM binding to the channel that persisted after patch excision, we repeated our experiments in the presence of CaM inhibitors. We tested several CaM inhibitors in inside-out patches, including ophiobolin A, W-7, and calmidazolium, which have been shown to regulate the sensitization of TRPV3 in whole cells (Xiao et al., 2008). Surprisingly, both ophiobolin A and W-7 showed similar effects to BAPTA in inside-out patches (Fig. 7), albeit to a lesser extent. They both potentiated the gating of the channel and accelerated the sensitization. Their potentiation effects were also reversible upon washout. However, another inhibitor, calmidazolium, showed no effect on either sensitization or potentiation of the channel in inside-out patches, contrary to its actions in whole cells. The differential effects of these inhibitors in excised patches have several implications. First, they suggest that the sensitization we observed in excised patches was unlikely mediated by Ca^{2+}–CaM. Second, some CaM inhibitors such as ophiobolin A and W-7 may directly interfere with the gating of TRPV3. Third, the CaM-dependent regulation remains a relevant mechanism of

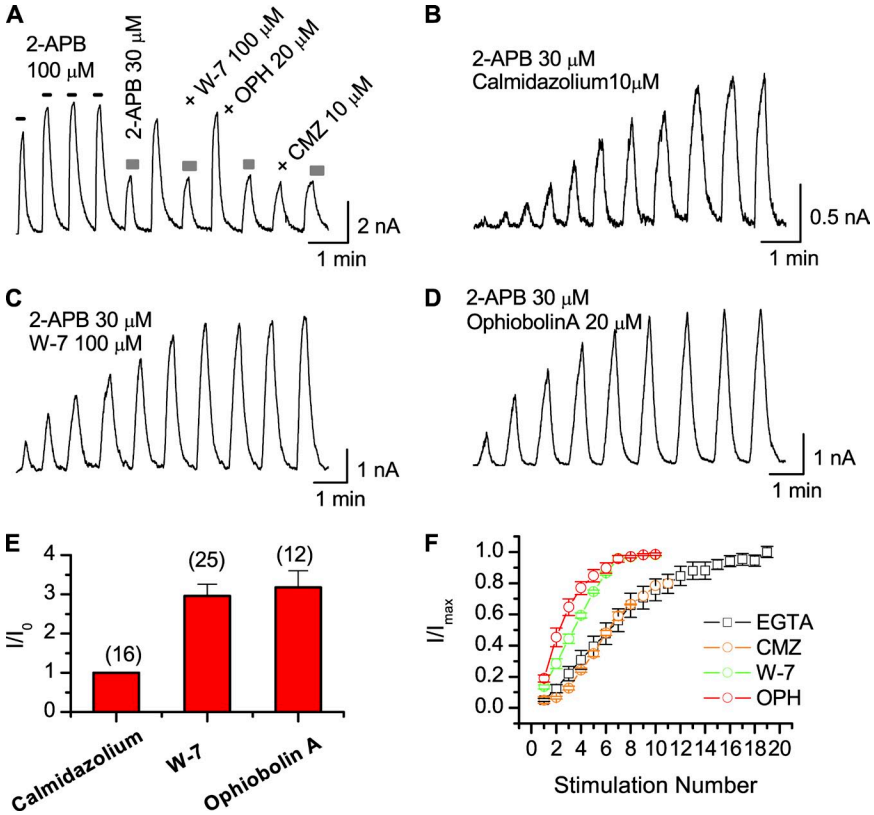

Figure 7. Effects of CaM inhibitors. (A) Ophiobolin A and W-7, but not calmidazolium, potentiates TRPV3. The channel was first sensitized by treatments with 100 μM 2-APB, followed by the application of 30 μM 2-APB in the absence or presence of CaM inhibitors to test for the effects of the inhibitors and their reversibility. (B–D) Ophiobolin A and W-7, but not calmidazolium, accelerate the sensitization of TRPV3 induced by 30 μM 2-APB. (E) Average plot for potentiation of 2-APB responses (30 μM). The relative increase of the current after the addition of CaM inhibitors is shown. (F) Time course of sensitization with or without CaM inhibitors. Currents were normalized by the maximum response after sensitization. Responses for calmidazolium were shown for the first 11 stimulation epochs only, because calmidazolium appeared to cause patch-seal deterioration, making long stable recording difficult. Data were recorded in inside-out patches at +60 mV.

sensitization in whole cells, as implied by the differential effects of calmidazolium in different patch configurations. It appears that the sensitization in intact cells involves both mechanisms: the membrane-delimited hysteresis of gating and the regulation by intracellular Ca^{2+} release. It is also possible that Ca^{2+}–CaM acts as a negative modulator, slowing down the rate of sensitization in a manner opposed to that of BAPTA and its benzene ring–containing analogues. In this case, neither Ca^{2+}–CaM nor BAPTA is a direct cause of hysteresis (which is intrinsic to TRPV3). Instead, they affect the kinetics of hysteresis through negative and positive modulation of channel gating, respectively.

Hysteresis occurs when the activation of a channel involves transitions that are slow relative to detection time. Most ion channels appear to be able to rapidly equilibrate between different conformations. Nevertheless, hysteresis has been observed for a few voltage-gated ion channels. For example, Shaker Kv and hyperpolarization-activated, cyclic nucleotide–gated channels both display a prepulse-dependent change in their Q-V relationships (Olcese et al., 1997; Männikkö et al., 2005). For Shaker, the change has been linked to the slow C-type inactivation resulting from structural changes in the outer pore region. For hyperpolarization-activated, cyclic nucleotide–gated channels, the hysteresis arises because of a slow shift between two gating modes. Another voltage-gated channel, the HERG-like K^+ channel, also shows hysteresis in the voltage dependence of opening when exposed to a common test pulse from different holding potentials (Pennefather et al., 1998; Zhou et al., 1998). The origin of the hysteresis was related to a slow inactivation component that takes minutes to equilibrate, thus leading to protocol-dependent changes in channel activity.

The hysteresis of TRPV3 differs from that of voltage-gated channels on some important aspects. One is that the hysteresis of TRPV3 occurs as though it is a perquisite step for the function of the channel. For example, the first heat treatment does not activate an appreciable channel activity at temperatures up to >50°C. A robust response occurs only after repeated stimulation of the channel. Similarly, the initial 2-APB treatment produces a small response at concentrations that are nearly saturating after the channel is sensitized (>100–300 μM). Another difference is that the hysteresis of TRPV3 occurs only before the channel is sensitized. After sensitization, the gating appears to be reversible. These features of hysteresis may be understood qualitatively with a simple state model as illustrated in Scheme 1 or 2 (the models differ in whether the channel returns to an intermediate closed state [Scheme 1] or a new resting [closed] state [Scheme 2] after opening). In these models, the rate constants k_0 and k_1 are driven by the stimulus. The return rate to C_0 is slow, so that the transition from C_0 to C_1 or O is irreversible. Thus, after stimulation, the occupancy of the channel is shifted from C_0 to C_1. The stimulus drives the channel away from the initial resting state. When the activation and deactivation rates (k_1 and k_2) of the channel are fast (relative to k_0), the occupancy in C_1 will determine the open probability of the channel in response to a brief stimulation. As the C_1 occupancy is gradually built up over repeated stimulation, the channel activity increases successively, thereby resulting in sensitization of the channel. So according to the models, the hysteresis occurs because of the nearly irreversible transition from C_0 to C_1/O, whereas the sensitization results from the accumulation of occupancy in the C_1 state. A reversible activation is reached when C_0 becomes fully depleted. As an illustration, we analyzed the sensitization of the channel with such models. Fig. 8 shows that both models were able to recapitulate the increase of the peak response upon repeated stimulation by 100 μM 2-APB. (We only fitted the peak response because our perfusion apparatus had a slow response time, inadequate to resolve the activation and deactivation time courses of the channel. The fitted activation and deactivation time courses appeared faster than the data, so the apparent time courses would be determined by that of the instrument.) In spite of the fit, the models are over-simplistic. For example, the channel is a tetramer, comprising multiple agonist binding sites. The sensitization at low agonist concentrations tends to have a sigmoidal time course (Figs. 1 and 2). To account for such features, these models need to be expanded, for example, by incorporating multiple kinetic steps for hysteresis and by replacing the single-step binding and gating (C_1-O) with a concerted multistep

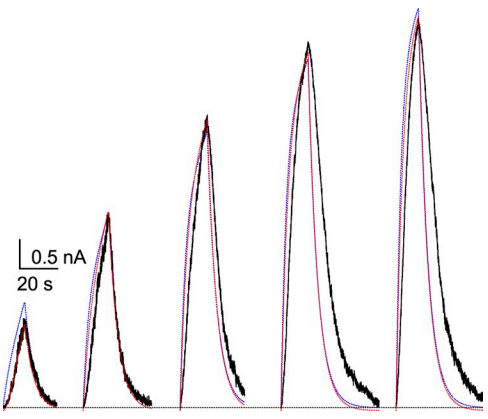

Figure 8. Analysis of sensitization by hysteresis-dependent models. Solid lines, data traces; dotted lines, model traces (red, Scheme 1; blue, Scheme 2). Data were repetitive 2-APB (100 μM) responses in an inside-out patch at +60 mV. The model was fit to the change of the peak currents. The time courses of activation and deactivation of the model were constrained to be faster than the data, so that the apparent time courses were that of the instrument (i.e., the perfusion apparatus). Fitted parameters (k_0, k_1, and k_2 in s^{-1}): 0.02, 0.1, and 0.2 (Scheme 1); and 0.01, 0.2, and 0.2 (Scheme 2). The hysteresis step was assumed to be irreversible.

binding and gating model to reflect the tetramer configuration of the channel. Despite the limitation, these models provide a starting point for conceptually understanding the likely complex activation and sensitization mechanisms of the channel.

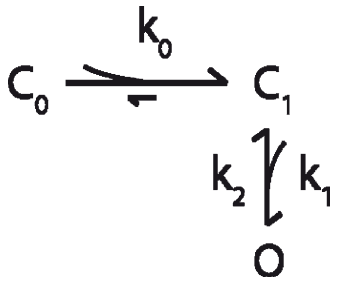

(SCHEME 1)

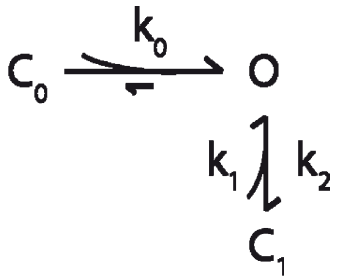

(SCHEME 2)

The two Ca^{2+} chelators BAPTA and EGTA differ mainly in their binding kinetics. Their binding affinities are similar. EGTA exists predominantly in the protonated form at physiological pH and has a relatively slow binding rate constant ($k_{on} = 1.5 \times 10^6/M \cdot s$), whereas BAPTA accelerates Ca^{2+} complexation ($k_{on} = 9.10^8/M \cdot s$) by preventing protonation at physiological pH. Although the difference in their effects has been mostly attributed to their distinct buffering kinetics and interpreted for the presence of localized fast Ca^{2+} rises, several reports have suggested that BAPTA can also exert pharmacological effects that are unrelated to its Ca^{2+}-binding properties. For example, BAPTA augments the peak current and shifts the voltage sensitivity of Ca^{2+} channels in bovine adrenal chromaffin cells (Bödding and Penner, 1999) and has potent effects on the gating of Cl^- channels (Sabanov and Nedergaard, 2007), whereas BAPTA-AM, which is membrane permeable, inhibits the hERG potassium channels (Tang et al., 2007). In rat sympathetic neurons, BAPTA interferes with the muscarinic signal transduction pathway, and the effect is independent of Ca^{2+} chelation (Beech et al., 1991). Dibromo-BAPTA inhibits exocytosis induced by guanosine 5′-O-(3-thiotriphosphate) (GTP[γ-S]) in rat peritoneal mast cells (Penner and Neher, 1988). In rat basophilic leukemia cells, BAPTA prevents the PKC-mediated inactivation of store-operated Ca^{2+} currents (Parekh and Penner, 1995). In most of these studies, the effects of BAPTA are specific and not conferred by even a high concentration of EGTA.

BAPTA is structurally different from EGTA with the addition of two benzene rings. Rousset et al. (2004) demonstrate that these hydrophobic moieties can cause BAPTA to directly interact with the plasma membrane, and such interactions are Ca^{2+} dependent because they occur only in its free form but not in the Ca^{2+}-bound form. As a result, BAPTA may act as a molecular shuttle to reduce the Ca^{2+} ions at the membrane surface. The potentiation effect of BAPTA on TRPV3, however, does not appear to require Ca^{2+}, suggesting that the Ca^{2+}-dependent insertion of BAPTA into membrane lipids is unlikely responsible. On the other hand, the structure of BAPTA is somewhat similar to 2-APB; they both possess di-benzene rings, a critical feature not shared by EGTA. In examining the importance of these hydrophobic moieties, we tested two synthetic dipeptides with a di-benzene ring structure but lacking Ca^{2+}-binding moiety. Both compounds were able to potentiate the channel and the effects were washable, similar to the effects of BAPTA. Thus, the effectiveness of these diverse compounds hints on a structure–function relationship involving the benzene rings.

We thank Philip Gottlieb for helpful discussions.

The work was supported by National Institutes of Health (grants R01-GM65994/84891) and Natural Science Foundation of China (grant 31028006). J. Yao was partially supported by a university fund (HUST 2011TS086).

Christopher Miller served as editor.

Submitted: 6 July 2011
Accepted: 21 September 2011

REFERENCES

Beech, D.J., L. Bernheim, A. Mathie, and B. Hille. 1991. Intracellular Ca2+ buffers disrupt muscarinic suppression of Ca2+ current and M current in rat sympathetic neurons. *Proc. Natl. Acad. Sci. USA.* 88:652–656. http://dx.doi.org/10.1073/pnas.88.2.652

Bödding, M., and R. Penner. 1999. Differential modulation of voltage-dependent Ca2+ currents by EGTA and BAPTA in bovine adrenal chromaffin cells. *Pflugers Arch.* 439:27–38. http://dx.doi.org/10.1007/s004240051124

Caterina, M.J., M.A. Schumacher, M. Tominaga, T.A. Rosen, J.D. Levine, and D. Julius. 1997. The capsaicin receptor: a heat-activated ion channel in the pain pathway. *Nature.* 389:816–824. http://dx.doi.org/10.1038/39807

Caterina, M.J., T.A. Rosen, M. Tominaga, A.J. Brake, and D. Julius. 1999. A capsaicin-receptor homologue with a high threshold for noxious heat. *Nature.* 398:436–441. http://dx.doi.org/10.1038/18906

Caterina, M.J., A. Leffler, A.B. Malmberg, W.J. Martin, J. Trafton, K.R. Petersen-Zeitz, M. Koltzenburg, A.I. Basbaum, and D. Julius. 2000. Impaired nociception and pain sensation in mice lacking the capsaicin receptor. *Science.* 288:306–313. http://dx.doi.org/10.1126/science.288.5464.306

Chung, M.K., H. Lee, A. Mizuno, M. Suzuki, and M.J. Caterina. 2004. 2-aminoethoxydiphenyl borate activates and sensitizes the

heat-gated ion channel TRPV3. *J. Neurosci.* 24:5177–5182. http://dx.doi.org/10.1523/JNEUROSCI.0934-04.2004

Davis, J.B., J. Gray, M.J. Gunthorpe, J.P. Hatcher, P.T. Davey, P. Overend, M.H. Harries, J. Latcham, C. Clapham, K. Atkinson, et al. 2000. Vanilloid receptor-1 is essential for inflammatory thermal hyperalgesia. *Nature.* 405:183–187. http://dx.doi.org/10.1038/35012076

Harks, E.G., J.P. Camiña, P.H. Peters, D.L. Ypey, W.J. Scheenen, E.J. van Zoelen, and A.P. Theuvenet. 2003. Besides affecting intracellular calcium signaling, 2-APB reversibly blocks gap junctional coupling in confluent monolayers, thereby allowing measurement of single-cell membrane currents in undissociated cells. *FASEB J.* 17:941–943.

Lis, A., C. Peinelt, A. Beck, S. Parvez, M. Monteilh-Zoller, A. Fleig, and R. Penner. 2007. CRACM1, CRACM2, and CRACM3 are store-operated Ca2+ channels with distinct functional properties. *Curr. Biol.* 17:794–800. http://dx.doi.org/10.1016/j.cub.2007.03.065

Männikkö, R., S. Pandey, H.P. Larsson, and F. Elinder. 2005. Hysteresis in the voltage dependence of HCN channels: conversion between two modes affects pacemaker properties. *J. Gen. Physiol.* 125:305–326. http://dx.doi.org/10.1085/jgp.200409130

Maruyama, T., T. Kanaji, S. Nakade, T. Kanno, and K. Mikoshiba. 1997. 2APB, 2-aminoethoxydiphenyl borate, a membrane-penetrable modulator of Ins(1,4,5)P3-induced Ca2+ release. *J. Biochem.* 122:498–505.

Moqrich, A., S.W. Hwang, T.J. Earley, M.J. Petrus, A.N. Murray, K.S. Spencer, M. Andahazy, G.M. Story, and A. Patapoutian. 2005. Impaired thermosensation in mice lacking TRPV3, a heat and camphor sensor in the skin. *Science.* 307:1468–1472. http://dx.doi.org/10.1126/science.1108609

Olcese, R., R. Latorre, L. Toro, F. Bezanilla, and E. Stefani. 1997. Correlation between charge movement and ionic current during slow inactivation in Shaker K^+ channels. *J. Gen. Physiol.* 110:579–589. http://dx.doi.org/10.1085/jgp.110.5.579

Parekh, A.B., and R. Penner. 1995. Depletion-activated calcium current is inhibited by protein kinase in RBL-2H3 cells. *Proc. Natl. Acad. Sci. USA.* 92:7907–7911. http://dx.doi.org/10.1073/pnas.92.17.7907

Peier, A.M., A.J. Reeve, D.A. Andersson, A. Moqrich, T.J. Earley, A.C. Hergarden, G.M. Story, S. Colley, J.B. Hogenesch, P. McIntyre, et al. 2002. A heat-sensitive TRP channel expressed in keratinocytes. *Science.* 296:2046–2049. http://dx.doi.org/10.1126/science.1073140

Pennefather, P.S., W. Zhou, and T.E. DeCoursey. 1998. Idiosyncratic gating of HERG-like K^+ channels in microglia. *J. Gen. Physiol.* 111:795–805. http://dx.doi.org/10.1085/jgp.111.6.795

Penner, R., and E. Neher. 1988. Secretory responses of rat peritoneal mast cells to high intracellular calcium. *FEBS Lett.* 226:307–313. http://dx.doi.org/10.1016/0014-5793(88)81445-5

Phelps, C.B., R.R. Wang, S.S. Choo, and R. Gaudet. 2010. Differential regulation of TRPV1, TRPV3, and TRPV4 sensitivity through a conserved binding site on the ankyrin repeat domain. *J. Biol. Chem.* 285:731–740. http://dx.doi.org/10.1074/jbc.M109.052548

Rousset, M., T. Cens, N. Vanmau, and P. Charnet. 2004. Ca2+-dependent interaction of BAPTA with phospholipids. *FEBS Lett.* 576:41–45. http://dx.doi.org/10.1016/j.febslet.2004.08.058

Sabanov, V., and J. Nedergaard. 2007. Ca(2+)-independent effects of BAPTA and EGTA on single-channel Cl(−) currents in brown adipocytes. *Biochim. Biophys. Acta.* 1768:2714–2725. http://dx.doi.org/10.1016/j.bbamem.2007.07.003

Smith, G.D., M.J. Gunthorpe, R.E. Kelsell, P.D. Hayes, P. Reilly, P. Facer, J.E. Wright, J.C. Jerman, J.P. Walhin, L. Ooi, et al. 2002. TRPV3 is a temperature-sensitive vanilloid receptor-like protein. *Nature.* 418:186–190. http://dx.doi.org/10.1038/nature00894

Tang, Q., M.W. Jin, J.Z. Xiang, M.Q. Dong, H.Y. Sun, C.P. Lau, and G.R. Li. 2007. The membrane permeable calcium chelator BAPTA-AM directly blocks human ether a-go-go-related gene potassium channels stably expressed in HEK 293 cells. *Biochem. Pharmacol.* 74:1596–1607. http://dx.doi.org/10.1016/j.bcp.2007.07.042

Xiao, R., J. Tang, C. Wang, C.K. Colton, J. Tian, and M.X. Zhu. 2008. Calcium plays a central role in the sensitization of TRPV3 channel to repetitive stimulations. *J. Biol. Chem.* 283:6162–6174. http://dx.doi.org/10.1074/jbc.M706535200

Xu, H., I.S. Ramsey, S.A. Kotecha, M.M. Moran, J.A. Chong, D. Lawson, P. Ge, J. Lilly, I. Silos-Santiago, Y. Xie, et al. 2002. TRPV3 is a calcium-permeable temperature-sensitive cation channel. *Nature.* 418:181–186. http://dx.doi.org/10.1038/nature00882

Xu, H., M. Delling, J.C. Jun, and D.E. Clapham. 2006. Oregano, thyme and clove-derived flavors and skin sensitizers activate specific TRP channels. *Nat. Neurosci.* 9:628–635. http://dx.doi.org/10.1038/nn1692

Yao, J., B.L. Liu, and F. Qin. 2010. Kinetic and energetic analysis of thermally activated TRPV1 channels. *Biophys. J.* 99:1743–1753. http://dx.doi.org/10.1016/j.bpj.2010.07.022

Zhou, W., F.S. Cayabyab, P.S. Pennefather, L.C. Schlichter, and T.E. DeCoursey. 1998. HERG-like K^+ channels in microglia. *J. Gen. Physiol.* 111:781–794. http://dx.doi.org/10.1085/jgp.111.6.781